



HHS Public Access

Author manuscript

J Chem Inf Model. Author manuscript; available in PMC 2019 May 29.

Published in final edited form as:

J Chem Inf Model. 2018 May 29; 58(5): 993–1004. doi:10.1021/acs.jcim.8b00132.

Polarizable Force Field for Molecular Ions Based on the Classical Drude Oscillator

Fang-Yu Lin^a, Pedro E. M. Lopes^a, Edward Harder^b, Benoît Roux^{b,†}, and Alexander D. MacKerell Jr.^{a,‡}

^aDepartment of Pharmaceutical Sciences, School of Pharmacy, University of Maryland, 20 Penn Street, Baltimore, MD 21201, USA

^bDepartment of Biochemistry and Molecular Biology, University of Chicago, Chicago, IL, 60637, USA

Abstract

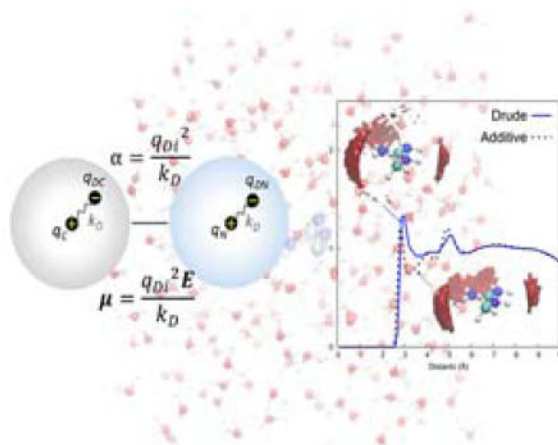
Development of accurate force field parameters for molecular ions in the context of a polarizable energy function based on the classical Drude oscillator is a crucial step towards an accurate polarizable model for modeling and simulations of biological macromolecules. Towards this goal we have undertaken a hierarchical approach in which force field parameter optimization is initially performed for small molecules for which experimental data exists that serve as building blocks of macromolecular systems. Small molecules representative of the ionic moieties of biological macromolecules include the cationic ammonium and methyl substituted ammonium derivatives, imidazolium, guanidinium and methylguanidinium and the anionic acetate, phenolate and alkanethiolates. In the present work, parameters for molecular ions in the context of the Drude polarizable force field are optimized and compared to results from the nonpolarizable additive CHARMM General Force Field (CGenFF). Electrostatic and Lennard-Jones parameters for the model compounds are developed in the context of the polarizable SWM4-NDP water model, with emphasis on assuring that the hydration free energies are consistent with previous reported parameters for atomic ions. The final parameters are shown to be in good agreement with the selected QM and experimental target data. Analysis of the structure of water around the ions reveal a substantial differences between the Drude and additive force fields indicating an important role of polarization in dictating the molecular details of aqueous solvation. The presented parameters represent the foundation for the charged functionalities in future generations of the Drude polarizable force field for biological macromolecules as well as for drug-like molecules.

Graphical abstract

^{†,‡}Corresponding author: roux@uchicago.edu; alex@outerbanks.umaryland.edu.

Conflict of Interest: Alexander D. MacKerell, Jr. is cofounder and CSO of SilcsBio LLC.

Supporting Information: The Supporting Information is available free of charge on the ACS Publications website. Tables showing calculation of target hydration free energies for the additive model, minimum water interaction distances and energies, internal geometries, and vibrational spectra of the molecular ions. Figures showing water radial distribution functions, additional water interaction energy surfaces and spatial probability distributions of water, and parameters for molecular ions developed under this study.



1. Introduction

Classical molecular dynamics (MD) simulations based on empirical force fields (FFs) are widely used in a broad range of scientific fields such as chemistry, biochemistry, biophysics, engineering, and materials science. In particular, MD simulations may be used to investigate the structure and dynamics of complex biological processes at the atomic level under a wide variety of conditions. Examples include studies of ligand binding, enzymatic-reaction mechanisms, protein or RNA folding and protein-protein interactions.¹

Central to the quality of the results from MD-based technologies is the accuracy of the underlying force field used to calculate the energies and forces acting on the system. As a result of many years of careful refinement, current additive biomolecular FFs have achieved a level of quality allowing them to be used to study dynamics, complex interactions and in pharmacological applications, among others.² However, limitations are present in the additive models. A simple example is the inability of such models to correctly treat the distribution of atomic ions at air-water interfaces,^{3–5} an issue that was overcome by the explicit inclusion of polarizability in the force field. Thus, it is clear that further improvements in the accuracy of macromolecular FFs will likely require the inclusion of electrostatic polarization, as induced fields from the solvent environment, including ions as well as the molecules of interest themselves will affect the electrostatic interactions.^{6–10}

Development of the Drude polarizable FF in the context of CHARMM,^{11, 12} subsequently extended to NAMD,^{13, 14} GROMACS,^{15, 16} and OpenMM,¹⁷ started in 2001 with optimization of the first water model (SWM4-DP).¹⁸ A later SWM4 water model was developed which included a negatively charged Drude particle, becoming the standard polarizable water model in the Drude polarizable FF (SWM4-NDP)¹⁹ and this has been followed by a six-point water model, SWM6-NDP,²⁰ which showed improvements in a number of properties, including the treatment of water clusters, though at an additional computational cost over the SWM4-NDP model. Development of the Drude polarizable FF continued with parametrization of small molecules covering the functional groups encountered in biomolecules, including alkanes,²¹ alcohols,²² aromatics,²³ among others.^{24–29} Development of parameters for N-methylacetamide (NMA) motivated extensions of

the Drude energy function to include anisotropic polarizabilities and atom-based Thole scale factors,³⁰ with the NMA model subsequently updated.³¹ More recently, Drude models for proteins,³² selected lipids^{33, 34} and carbohydrates^{28, 35–37} and DNA^{38, 39} have been presented. These are referred to as the Drude-2013 FF, with a second generation DNA force field,^{40, 41} along with the required parameters for RNA (Lemkul and MacKerell, Work in progress), referred to as Drude-2017 recently presented.

The molecular ions included in Drude-2013 FF were optimized to be consistent with published Drude parameters for atomic ions,⁴² though the details of the molecular ion parametrization were not presented. Moving ahead as part of the second generation Drude force field we have undertaken additional optimization of the Drude molecular ions. In the present study we provide a description of the parametrization of selected small molecule ions. Results on the performance of the FF in reproducing intramolecular geometries and vibrational spectra, interactions with water, dipole moments and molecular polarizability tensors based on quantum mechanical (QM) data, and experimental hydration free energies of the molecular ions are presented and discussed. The molecular ions considered in this study are listed in Table 1 along with their abbreviations. These were selected to cover the common ionic moieties in biological macromolecules at physiological pH, as well as the charged functionalities with pKa values close to physiological pH. Parameters for phosphate containing species will be presented as part of our ongoing efforts in the development of next generation nucleic acid and lipid force fields. Details of the Drude energy function and general parameter optimization strategies have been reported elsewhere^{43, 44} and are not presented in this report.

2. Computational Methods

QM calculations were performed with the PSI4⁴⁵ and Gaussian 03 programs.⁴⁶ Gas phase geometry optimizations were done at the MP2/aug-cc-pVDZ level. Vibrational frequencies were calculated using the optimized geometry with the same model chemistry. A scaling factor 0.959, obtained from the NIST Computational Chemistry Comparison and Benchmark Database,⁴⁷ was used to account for limitations in the level of theory.⁴⁸ A symbolic potential energy distribution (PED) analysis was performed as proposed by Pulay *et al.*⁴⁹ using the MOLVIB module in CHARMM¹² to obtain the vibrational frequencies and assignments. QM electrostatic potential (ESP) calculations were performed on the gas-phase MP2/aug-cc-pVDZ optimized geometries using the B3LYP hybrid functionals^{50–52} and the correlation-consistent double- ζ Dunning aug-cc-pVDZ basis set.⁵³ Interaction energies of the model compounds with water were performed using the QM gas phase model compound and SWM4-NDP or TIP3P internal geometries at the MP2/cc-pVQZ model chemistry including the basis set superposition error correction of Boys and Bernardi.⁵⁴ The calculations involved scans of the water to model compound distances in selected orientations (Figure 1 and Figure S1–S6) with the monomer geometries constrained to those obtained in the gas phase.

Empirical FF calculations were performed with the program CHARMM.¹² All calculations were performed with the SWM4-NDP¹⁹ water model as this is the default water model in the Drude force field due, in part, to its computational efficiency over the SWM6 model.²⁰

Additive force field calculations used the CHARMM General Force Field (CGenFF) parameters⁵⁵ along with the CHARMM TIP3P water model.⁵⁶ Gas phase optimizations included all possible nonbond interactions and were performed to a convergence threshold of 10^{-5} kcal·mol⁻¹·Å⁻¹ for the forces. Interactions with water used gas phase geometries in interaction orientations identical to those used in the QM calculations with the interaction energies obtained by taking the energy difference between the water-model complex and the water and model compound monomers, following relaxation of the Drude particles via a minimization by steepest-descent (SD) algorithm for 200 steps followed by an adopted-basis Newton-Raphson (ABNR) algorithm for 500 steps to a final gradient of 10^{-5} kcal·mol⁻¹·Å⁻¹ with the atomic positions restrained with a force constant of 10^7 kcal/mol/Å².

The hydration free energy of molecular ions was calculated through alchemical free energy perturbation (FEP) simulations.⁵⁷ Final hydration free energies were based on three individual calculations, as described below. In addition, to study the structure and dynamics of the hydrated ions to recover the full layered structure of the water, the cubic box of 250 water molecules and a single ion was submitted to a 10 ns simulation for each molecular ion for analysis of the radial distribution functions and 3D spatial probability distributions of water.

Simulations of the ions in aqueous solution were performed with cubic periodic boxes containing 250 water molecules and a single molecular ion restrained to the center of the simulation box through a force constant of 0.5 kcal/(mol·Å²) on the center of mass of all solute real atoms. Simulations were performed at 298.15 K and 1 atm pressure, corresponding to the experimental conditions. MD simulations of the Drude models were performed using the extended Lagrangian formalism implemented in CHARMM,^{18, 58} with a mass of 0.4 AMU subtracted from the polarizable atoms (ie. nonhydrogens) and assigned to the Drude particles. The time step used in all simulations was 1 fs for the Drude model and 2 fs for the additive model. Long-range electrostatic interactions were computed using particle mesh Ewald summation⁵⁹ with a real space cutoff of 12 Å, Ewald splitting parameter of 0.34 Å⁻¹, a grid spacing of ~ 1.0 Å, and a sixth-order interpolation of the charge to the grid was used. Lennard-Jones (LJ) 6–12 term parameters were truncated at 12 Å with switch smoothing⁶⁰ used for the Drude and force switch smoothing⁶¹ for the additive applied between 10 and 12 Å. Simulations in the isothermal–isobaric ensemble used a Nosé–Hoover thermostat^{62, 63} and the modified Andersen–Hoover barostat of Martyna et al.⁶⁴ The internal geometry of the SWM4-NDP water molecule and covalent bonds involving hydrogens were kept rigidly fixed using the SHAKE/Roll and RATTLE/Roll algorithm.^{65, 66} Gas-phase simulations were carried out using Langevin Dynamics with a friction constant of 5 ps⁻¹.

The computation of hydration free energies of charged species is more complex than with neutral compounds because it must also account for the contribution arising from the Galvani potential Φ originating from the vacuum/water interface.^{67–69} Accordingly, we define the ‘real’ hydration free energy $\Delta G_{\text{hyd}}^{0, \text{real}}$ as the total reversible work to physically transfer a charged species from the gas phase to the bulk solvent phase (crossing the physical air/water interface).^{69–71}

$$\Delta G_{\text{hyd}}^{0,\text{real}} = \Delta G_{\text{hyd}}^{0,\text{intr}} + zF\Phi \quad \text{Eq. 1}$$

In equation 1, z is the charge of the species, F is the Faraday constant (23.06 kcal/mol/V), Φ is the phase potential of water relative to vacuum or the electrostatic Galvani potential at the vacuum/water interface, and $\Delta G_{\text{hyd}}^{0,\text{intr}}$ is referred to as the ‘intrinsic’ free energy. Although the real free energy $\Delta G_{\text{hyd}}^{0,\text{real}}$ is physically invariant, both Φ and $\Delta G_{\text{hyd}}^{0,\text{intr}}$ depend on the choice of mathematical convention. While Φ cannot be measured experimentally by a physical process, “internal” or “external” Galvani potentials may be defined mathematically unambiguously by specifying the convention used in the calculation (P- or M-sum).⁶⁸ As discussed by Kastenholz and Hünenberger,^{72, 73} the convention for summing up the contributions of solvent charges to the electrostatic potential in the aqueous phase can be made based on point charges within entire solvent molecules (M-sum) or on the basis of individual point charges (P-sum). In the present work, the calculated free energies rely on periodic boundary conditions (PBC) and the particle mesh Ewald (PME) method carried out within the P-sum convention, and the implicit reference phase potential Φ of the liquid is the “internal” Galvani potential. The results from FEP simulations with PBC/PME are the intrinsic free energies, $\Delta G_{\text{hyd}}^{0,\text{intr}}$, which then need to be corrected by $zF\Phi$ (with Φ calculated within the same P-sum convention) to yield the physically meaningful $\Delta G_{\text{hyd}}^{0,\text{real}}$. For the polarizable SWM4-NDP water model, the P-sum internal Galvani potential Φ is equal to -545 mV¹⁹ (negative in the liquid phase relative to vacuum), giving rise to an energy shift of $zF\Phi$ being ± 12.6 kcal·mol⁻¹ for the monovalent cations/anions.¹⁹ For the additive TIP3 water model, Φ is equal to -500 mV such that $zF\Phi$ is ± 11.5 kcal/mol.⁶⁹

Following the previously reported Deng and Roux protocol,⁷⁴ the total solvation free energy (G_{tot}) is calculated as a sum of the differences between gas and aqueous-phase system vdW repulsive (G_{rep}), vdW dispersive (G_{disp}) and electrostatic (G_{elec}) terms as shown in equation 2.

$$\Delta G_{\text{tot}} = \Delta G_{\text{rep}} + \Delta G_{\text{disp}} + \Delta G_{\text{elec}} \quad \text{Eq. 2}$$

In the free energy perturbation protocol, the gas and aqueous-phase simulations used the same coupling parameter schemes. The repulsive contribution (G_{rep}) was computed using a soft-core scheme⁷⁴ with the staging parameter, s , set to 0.0, 0.2, 0.3, 0.4, 0.5, 0.6, 0.7, 0.8, 0.9, and 1.0. The electrostatic (G_{elec}) and dispersive (G_{disp}) components were calculated using the standard linear coupling scheme with coupling parameters λ and ξ , varying from 0 to 1 with the increments of 0.1. For each window, a 50 ps equilibration and a 400 ps production simulation were performed. The weighted histogram analysis method (WHAM)⁷⁵ was used for computing nonpolar contributions to the free energy difference while the electrostatic contributions were computed using thermodynamic integration (TI). A long-range correction (LRC)⁷⁶ was then included in the calculation of $\Delta G_{\text{hyd}}^{0,\text{intr}}$, where the

LRC is the difference when the LJ solvent-solute interaction energies use cutoff schemes of 12 and 50 Å. Thus, the $\Delta G_{\text{hyd}}^{0,\text{real}}$ are computed from the sum of $\Delta G_{\text{hyd}}^{0,\text{intr}}$, the entropic contribution of $+1.9 \text{ kcal}\cdot\text{mol}^{-1}$,^{42, 69} and $zF\Phi$. The real free energy $\Delta G_{\text{hyd}}^{0,\text{real}}$ is commonly referred to as “absolute” solvation free energy to draw a clear distinction with relative free energy between two different ions, although in physical terms, it corresponds to the reversible thermodynamic work to move the ion from vacuum to the bulk water phase. While such an absolute solvation free energy can be calculated unambiguously, in practice, only relative free energies of ions of the same charge or of neutral salts can actually be measured experimentally. In spite of this, experimental values of charged species are often reported as if they are absolute values, although they always depend on an arbitrary offset that may differ between the various reports. The offset is sometimes reported in terms of the absolute hydration free energy of a proton, but this information is not always provided explicitly. The confusion has been further compounded at times by the concepts of “intrinsic” and “real” solvation free energy (see discussion above). Accordingly, one cannot rely naïvely on absolute experimental values because there is no unambiguous reference scale for charged species. All experiments have to utilize some reference scale. Thus, special caution is needed when combining experimental values taken from different studies; a simple subtraction of two absolute values from two different studies does not yield a valid relative free energy since both studies may not have assumed the same implicit offset. This issue is important in force field development because the absolute hydration free energies of the different ions must be internally consistent, for example, to accurately account for the relative binding and ion-pairing affinities. To resolve this issue, let us assume that one knows from experiment the absolute experimental solvation free energy of a negatively charged compound with a charge of -1 . There are essentially two methods to combine the experimental values from different studies to obtain the target data for the present optimization. These take advantage of hydration free energy of Cl^- and Na^+ and reference H^+ used in the previous development of the Drude monoatomic ions⁴² (Table 2), which will be used to normalize the hydration free energies for the molecular ions, $\text{Y}^{+/-}$, reported in the literature.⁷⁷⁻⁸¹ Method 1 is used when the reference is a co-ion of the same charge (eg. Cl^- as the reference in the case of CH_3COO^- , or Na^+ in the case of NH_4^+). Method 2 is used when the reference is based on a counterion for forming a neutral salt (eg. Na^+ or H^+ in the case of CH_3COO^- , or Cl^- in the case of NH_4^+). We note that Hofer and Hünenberger have recently developed a QM/MM based approach to calculate the accurate proton solvation free energy,⁸² though this result is not relevant to the present study.

Method 1—Let us assume the molecule is CH_3COO^- . If the literature reports $G_{\text{hyd}}(\text{Cl}^-_{\text{ref}})$ and $G_{\text{hyd}}(\text{CH}_3\text{COO}^-_{\text{ref}})$, then the difference of $G_{\text{hyd}}(\text{Cl}^-_{\text{ref}})$ and $G_{\text{hyd}}(\text{CH}_3\text{COO}^-_{\text{ref}})$ will be used to determine the absolute scale. As $G_{\text{hyd}}(\text{Cl}^-_{\text{Drude}})$ is -78.4 kcal/mol ,⁴² the target $G_{\text{hyd,target}}$ value for CH_3COO^- will be $-78.4 \text{ kcal/mol} + G_{\text{hyd}}(\text{CH}_3\text{COO}^-_{\text{ref}}) - G_{\text{hyd}}(\text{Cl}^-_{\text{ref}})$. The same method also applies to cationic molecules. This calculation is described in equation 3.

$$\begin{aligned} \Delta G(Y^{-/+}_{\text{ref}}) - \Delta G(X^{-/+}_{\text{ref}}) &= \Delta G(Y^{-/+}_{\text{target}}) - \Delta G(X^{-/+}_{\text{Drude}}) = > \Delta G(Y^{-/+}_{\text{target}}) \\ &= \Delta G(X^{-/+}_{\text{Drude}}) + \Delta G(Y^{-/+}_{\text{ref}}) - \Delta G(X^{-/+}_{\text{ref}}) \end{aligned}$$

Eq. 3

Method 2—Again let us assume the molecular ion is acetate and the literature reports

$G_{\text{hyd}}(\text{Na}^+_{\text{ref}})$ and $G_{\text{hyd}}(\text{CH}_3\text{COO}^-_{\text{ref}})$. Then, the sum of $G_{\text{hyd}}(\text{Na}^+_{\text{ref}})$ and $G_{\text{hyd}}(\text{CH}_3\text{COO}^-_{\text{ref}})$ will be used to determine the absolute scale. As the $G_{\text{hyd}}(\text{Na}^+_{\text{Drude}})$ is -96.3 kcal/mol,⁴² the target $G_{\text{hyd,target}}$ value for CH_3COO^- will be $G_{\text{hyd}}(\text{Na}^+_{\text{ref}}) + G_{\text{hyd}}(\text{CH}_3\text{COO}^-_{\text{ref}}) - (-96.3$ kcal/mol). The same method also applies to cationic molecules. This calculation is described in equation 4.

$$\begin{aligned} \Delta G(X^{-/+}_{\text{ref}}) + \Delta G(Y^{-/+}_{\text{ref}}) &= \Delta G(X^{-/+}_{\text{Drude}}) + \Delta G(Y^{-/+}_{\text{target}}) = > \Delta G(Y^{-/+}_{\text{target}}) \\ &= \Delta G(X^{-/+}_{\text{ref}}) + \Delta G(Y^{-/+}_{\text{ref}}) - \Delta G(X^{-/+}_{\text{Drude}}) \end{aligned}$$

Eq. 4

In equations 3 and 4, $G(Y^{-/+}_{\text{ref}})$ is the hydration free energies for the molecular ions, $Y^{+/-}$, reported in the literature, $G(X^{-/+}_{\text{ref}})$ is the hydration free energies for ions, $X^{+/-}$, reported in the literature, $G(Y^{-/+}_{\text{target}})$ is the target hydration free energies for the molecular ions obtained from the Drude force field and $G(X^{-/+}_{\text{Drude}})$ is the hydration free energies for the ions obtained from Drude or reference H^+ used in the development of the Drude monoatomic ions (Table 2).

Finally, while the shifting of the relative scales is simple in the case of monovalent ions, it requires more caution in the case of divalent ions. In this case, forming the neutral salt is the safest way to avoid mistakes. For example, assume that your compound (X^{2-}) is negative with a charged of -2 with a reported hydration free energy of $\Delta G_{\text{X}^{2-}}^{\text{exp}}$ in the literature. If the report provides the hydration free energy of another cation like Na^+ , $\Delta G_{\text{Na}^+}^{\text{exp}}$, then one can use this to determine the absolute scale of $\Delta G_{\text{X}^{2-}}^{\text{FF}}$ for X^{2-} by forming a neutral salt with two Na^+ ,

$$\Delta G_{\text{X}^{2-}}^{\text{FF}} = \left[\Delta G_{\text{X}^{2-}}^{\text{exp}} + 2\Delta G_{\text{Na}^+}^{\text{exp}} \right] - 2\Delta G_{\text{Na}^+}^{\text{FF}}. \quad \text{Eq. 5}$$

This reasoning can be generalized to charged species of arbitrary valence. Based on the above correction schemes the target hydration free energies along with the various correction values are shown in Table 3. Analogous data for the additive CGenFF force field is presented in Table S1 of the supporting information.

3. Results and Discussion

3.1 Parametrization strategy

Development of parameters for the Drude FF in CHARMM follows the previously described iterative methodology.^{20,23} For example, the initial electrostatic, internal and LJ parameters are used to calculate the free energies of hydration. Based on those values as well as considering the remaining target data, changes in, for example, the electrostatic parameters are performed followed by analysis of the remaining target data, re-evaluation of the free energy of hydration and so on. Accordingly, when any of the parameters were adjusted all remaining target data was recalculated and additional adjustments of the parameters made was required. The following results are based on the final set of parameters, which will be accessible from the MacKerell laboratory web site (http://mackerell.umaryland.edu/CHARMM_ff_params.html), with future releases of the program CHARMM and from the Drude Prepper module in the CHARMM-GUI.⁸³

Electrostatic parameters in the polarizable Drude model include partial atomic charges, atomic polarizabilities, and atom-based Thole scale factors.^{84, 85} In addition, selected hydrogen bond acceptor atoms include anisotropic corrections to their polarizabilities as well as virtual particles representative of lone pairs (LP).⁸⁵ Initial determination of the electrostatic parameters is based on a series of ESPs surrounding the model compound determined using QM density functional theory on a set of specified grid points, differing by the presence and location of a perturbing charge in the environment surrounding the molecule.^{10, 84} Electrostatic parameters are then fitted to minimize the difference between the QM and Drude ESP maps. Initial guesses for the electrostatic parameters were taken from the neutral analogues of each molecular ion. Initial polarizabilities were the atomic hybrid polarizability values published by Miller.⁸⁶ Subsequently, iterative optimization of the electrostatic parameters, in conjunction of the optimization of the remaining parameters (see below), involved manual adjustments targeting dipole moments, molecular polarizabilities, interactions with water and hydration free energies.

Optimization of the remaining components of the FF, namely the internal and LJ terms, were adjusted as described previously for the additive CHARMM FF.^{87, 88} Internal parameters were optimized by targeting experimental and QM data that included geometries, vibrational spectra and conformational energies. Optimization of LJ parameters, which model vdW forces in the Drude FF, rely on reproduction of experimental hydration free energies (Table 3). In addition, QM minimum interaction energies and distances of the model compounds with water are used as LJ target data (Table S2).

3.2 Electrostatic and LJ Parameters

Partial atomic charges, atomic polarizabilities, and Thole scale factors were initially optimized targeting QM ESPs. Target molecular polarizabilities were not scaled in the cations and scaled by 0.6 to 0.7 for the anions, a value similar to that used for the SWM4-NDP water model¹⁹ and for the Drude alcohols.²² In ACET, MES and ETS the positions of LPs were manually adjusted to improve agreement between the Drude FF and QM calculated interactions with water. With PHET the quality of the model in the absence of the LPs was deemed adequate based on reproduction of QM interactions with water and the free energy of hydration such that LPs are not included in that model.

Initial values for the LJ parameters were based on neutral analogs of the molecular ions with adjustments first based on the reproduction of QM minimum interaction energies and distances between the ions and water. The interaction orientations between water and the protonated amines are shown in Figure 1 along with the QM, Drude and additive CGenFF interaction energy surfaces. Similar images and data for all the molecules considered in this study are shown in Figures S1 to S6 of the supporting information. It should be noted that the interactions were treated individually (e.g. as monohydrates). A summary of the model compound-water interaction energy results is shown in Table 4, with the data for the individual interactions presented in Table S2 of the supporting information. Overall, good agreement between QM and MM reported minimum interaction distance and energies are observed. The minimum interaction distances are systematically longer in the Drude model and the interaction energies are slightly less favorable. The average distance and energy differences are better with the additive CGenFF force field though the variation is larger, which is also seen in the larger AUE and RMSD values with the additive model. The overall level of agreement with the Drude model, whose parameters were optimized as part of the present study, was partially compromised due to the LJ parameters also being optimized to reproduce the hydration free energies. Results of the hydration free energy analysis are presented below.

Dipole moments of the model compounds were also considered during optimization of the electrostatic parameters. Presented in Table 5 are the QM dipole moments along with Drude and additive values. In general, the Drude values are in good agreement with the QM data. The differences with the additive model are systematically larger as expected given that the QM data was not considered when optimizing that model. We note that the impact of the dipole moment on interactions with the environment is less important with charged species vs. polar, neutral compounds as the monopole on the ions dominates such interactions.

An important quality of a polarizable FF is to accurately represent the molecular polarizability tensors, which determine the magnitude of the induced dipoles in the presence of an electric field. Thus, the polarizability tensors of all model compounds were computed and compared to QM values. Only the diagonal elements of the polarizability tensors are non-zero due to the alignment of each molecular ion along the axis of inertia. The components of the polarizability tensor along each coordinate axis were computed from finite-difference of the respective dipole moment component, x, y or z, in the presence and absence of an applied electrical field of 10^{10} V/m, respectively, parallel to the x, y, or z directions. Comparison of the QM reference values and equivalent quantities calculated with

the polarizable Drude model is presented in Table 6. Overall, the discrepancies between the polarizable Drude model and QM values are small, evidencing the ability of the polarizable model to reproduce subtle aspects of the electrostatic behavior of the molecules under study. With polar neutral species in the Drude force field it has been shown that the polarizabilities need to be scaled by values down to 0.6 in order to reproduce the dielectric constants of pure solvents.²⁷ In the present study the interactions with water, reproduction of dipole moments and reproduction of experimental hydration free energies were used to optimize electrostatic parameters. This approach revealed that there was no need to scale the polarizabilities of ammonium and the methylated derivatives of ammonium as good reproduction of the hydration free energies was achieved (see below). However, polarizability scaling was required with guanidinium, methylguanidinium and the anions. The scale factor of 0.85/0.86 used with GUAN, MGUAN and ACET falls in the range of scaling values obtained with the polar neutral species. With PHET and the sulfur containing compounds scale factors of 0.6 were required. This value is consistent with that determined for neutral sulfur containing compounds,²⁷ though the value of 0.64 for PHET is lower the values in the range of 0.7 used for neutral alcohols.²²

3.3 Internal geometries and vibrational spectra

Parameters for the bonds, valence angles and dihedral angles were optimized to reproduce QM optimized geometries and vibrational spectra of the studied molecular ions. Internal parameters for the methyl groups in ACET and the methylated derivatives of ammonium and guanidinium were transferred from the alkanes.²¹ Target data for the geometries included the optimized structure of the compounds at the MP2/aug-cc-pVDZ level. RMS differences of the bonds and angles with respect to the target data are shown in Table 7. The absolute values of all bond distances and angles and comparison with the QM data are shown in Table S3 of the Supporting Information. The agreement between calculated and target values is in general good, falling within the targeted differences of 0.02 Å for bonds and ~2° for angles, a level of agreement that is commonly used for the CHARMM FFs.^{2, 87, 89}

One of the distinctive features of the CHARMM additive and Drude force fields is the use of reproduction of QM vibrational frequencies within the harmonic approximation to optimize the empirical force constants. Emphasis was placed on the magnitude of the frequencies along with the reproduction of the assignments. All vibrational frequencies and assignments for the model compounds are shown in Table S4 of the Supporting Information. Overall, the agreement for the lowest frequency vibrational modes between the QM and MM models is quite good, indicating that the Drude force field will satisfactorily treat structural variations of the ions that occur during MD simulations.

3.4 Free Energies of Hydration

Central to the quality of a force field for ions is its accuracy with respect to estimation of hydration free energies, with those estimates based on common offset of the free energies as discussed above. Proper offset of the hydration free energies is essential to assure that the relative hydration free energies of all ions in the force field are correct. Statistical analysis of the results for the presented Drude model and CGenFF are shown in Table 8 with the results for the individual ions shown in Table 9. With the exception of NH₄, the calculated

hydration free energies for the Drude model are within 2 kcal/mol of the experimental target values. Substantially larger differences occur with CGenFF leading to the larger AVG, AUE and RMSD values with the additive model. This larger discrepancy is expected due to the additive force field parameters primarily being optimized based on QM interactions with water, where the QM calculations were performed at the HF/6-31G* model chemistry, consistent with that used for CGenFF and the entire C36 additive force field.^{2, 55} However, the ordering of the hydration free energies with the additive force field is quite acceptable, as is that for the Drude model as seen in Figure 2 and in the R^2 values in Table 8. This indicates the potential utility of both force fields in predicting the relative hydration energies of the molecular ions in different chemical contexts.

With the Drude force field the discrepancy with NH₄ (ammonium) is based on the optimization focusing on the methylated ammonium analogs (NC1 through NC4), such that the same LJ parameters are used for NH₄ and NC1 and for NC2 through NC4. Specific optimization of LJ parameters for NC1 ($\epsilon = -0.025$, $R_{\min/2} = 1.55$) yielded a calculated $G_{\text{hyd}}^{\text{real}}$ of -72.6 kcal/mol, in excellent agreement with target value in Table 9. An improved $G_{\text{hyd}}^{\text{real}}$ for NH₄ of -81.3 kcal/mol is obtained if LJ parameters ($\epsilon = -0.025$, $R_{\min/2} = 1.76$) specifically optimized for NH₄ are used. Concerning NC2 through NC4, the $G_{\text{hyd}}^{\text{real}}$ values of NC2 and NC3 are not favorable enough while NC4 is too favorable, a compromise that was deemed acceptable in the context of a single N atom type for the three compounds. With GUAN and the methyl analog, MGUAN, emphasis was placed on the methylated species as this is a better model for the side chain of Arginine. However, the discrepancy with GUAN is less than 2.0 kcal/mol, which is considered acceptable in the context of the same atom types. Overall, the presented Drude parameters for the molecular ions yield calculated hydration free energies that are in excellent agreement with experiment for the biomolecular-related ions included in this study.

3.5 Ion-Water coordination structure

Given the difference in the underlying potential energy function in the Drude polarizable and CGenFF additive force fields, radial distribution functions (RDFs) for the ions with water were calculated to determine if difference in the water structure is present between the two models. RDFs were extracted from 10 ns simulations of the single ions immersed in a box of water, with the results presented in Figures S7–S8 for molecular cations and anions, respectively. The resulting RDFs, shown in Figures S7–S8 show the overall structures of water around the ions to be similar for the two models. However, differences are present and, interestingly, consistent trends in those difference are largely not present. For example with NC1, the first peak is higher with CGenFF while the opposite is true with NC2, NC3 and NC4. With GUAN and MGUAN, the RDFs are smooth at 3–4 Å with the Drude model (Figure S7). With the anions, subtle changes occur in the first peak and a trend occurs where the second peak is systematically larger with the Drude force field (Figure S8).

Given the subtle differences in the RDFs, more detailed analysis was undertaken involving the calculation of the 3D spatial probability distributions of water around the ions. Results in Figures 3–5 and S9–S13 do show obvious differences in most of the systems. For example, with NH₄ and the methylated ammonium analogs (NC1 through NC4) the water

distributions are less localized in the Drude model (Figure 3 and S9–S11). With GUAN and MGUAN, small water distributions occur above and below the planes of the molecules in the Drude model but are absent in additive model. With ACET, the water around the oxygens in the Drude model are more distributed and correspond to the lone pair directions (Figure 4a–b), which is likely associated with the use of lone pairs on the oxygens for better describing the directional hydrogen bonds. With PHET, the water distributions are more obvious on the external side of oxygen along the C–O bond in the Drude model (Figure 4c–d), showing that they are more favored around the negatively charged oxygen than in the additive model. Thus, while the two models yield generally similar solvation structures based on RDFs, differences are evident from the 3D spatial water distributions indicating the impact of the Drude model on solvation structure. Future efforts that compare calculated solvation structures with scattering studies of salt solutions are required to better evaluate the quality of the force fields with respect to their modeling of water structure.

4. Summary

Presented are classical Drude polarizable FF parameters of individual molecular ions that represent building blocks of larger molecules of biological interest such as peptides, lipids and carbohydrates. Contrary to neutral compounds, where extensive condensed phase properties are available, and against which newly developed parameters can be tested, for molecular ions such data is scarce. Moreover, when it is available, as with experimental Gibbs free energies of hydration, there are significant assumptions in deriving such data.⁹⁴ The fact that ions cannot exist alone or undergo phase transfer without a counter-ion is the primary complication in obtaining this data. To overcome this issue, we offset the hydration free energies in a consistent fashion thereby assuring that the relative hydration free energies are consistent throughout the force field. In the case of the Drude force field this was done to assure consistency with previously reported atomic ions.⁴² Similar corrections were applied to the additive CGenFF force field, with results from the model presented for comparison with the developed Drude molecular ions.

With respect to model development, special care was taken in optimizing the electrostatic and LJ parameters to assure a proper balance of local and condensed phase properties. This included assuring that the balance of interactions with water in different model compound-water orientations were satisfactorily reproduced as were dipole moments and molecular polarizabilities. Care was also taken to assure that the intramolecular geometries and the vibrational frequency distributions were in good agreement with QM target data. Finally, the Drude model is shown to reproduce hydration free energies at a high level of accuracy, with improvements over the additive CGenFF evident, though it is anticipated that improvements in the additive model could be made with optimization of the model undertaken. These results indicate that the Drude polarizable model of molecular ions is of satisfactory quality for use in molecular modeling and simulation studies.

Supplementary Material

Refer to Web version on PubMed Central for supplementary material.

Acknowledgments

Financial support from the NIH (GM072558 and GM070855) and computational support from the University of Maryland Computer-Aided Drug Design Center, and the Extreme Science and Engineering Discovery Environment (XSEDE), which is supported by National Science Foundation grant number OCI-1053575, are acknowledged. We thank Drs. Xiao Zhu and Chris Baker for helpful discussions.

References

- Karplus M, McCammon JA. Molecular dynamics simulations of biomolecules. *Nat Struct Biol.* 2002; 9:646–652. [PubMed: 12198485]
- MacKerell AD Jr. Empirical force fields for biological macromolecules: overview and issues. *J Comput Chem.* 2004; 25:1584–1604. [PubMed: 15264253]
- Jungwirth P, Tobias DJ. Molecular Structure of Salt Solutions: A New View of the Interface with Implications for Heterogeneous Atmospheric Chemistry. *J Phys Chem B.* 2001; 105:10468–10472.
- Chang T-M, Dang LX. Recent Advances in Molecular Simulations of Ion Solvation at Liquid Interfaces. *Chem Rev.* 2006; 106:1305–1322. [PubMed: 16608182]
- Jungwirth P, Tobias DJ. Specific Ion Effects at the Air/Water Interface. *Chem Rev.* 2006; 106:1259–1281. [PubMed: 16608180]
- Warshel A, Kato M, Pisliakov AV. Polarizable force fields: History, test cases, and prospects. *J Chem Theory Comput.* 2007; 3:2034–2045. [PubMed: 26636199]
- Stone AJ. Intermolecular potentials. *Science.* 2008; 321:787–789. [PubMed: 18687950]
- Freddolino PL, Harrison CB, Liu YX, Schulten K. Challenges in protein-folding simulations. *Nat Phys.* 2010; 6:751–758. [PubMed: 21297873]
- Lopes PEM, Roux B, MacKerell AD Jr. Molecular modeling and dynamics studies with explicit inclusion of electronic polarizability: theory and applications. *Theor Chem Acc.* 2009; 124:11–28. [PubMed: 20577578]
- Zhu X, Lopes PEM, MacKerell AD Jr. Recent developments and applications of the CHARMM force fields. *Wiley Interdiscip Rev Comput Mol Sci.* 2012; 2:167–185. [PubMed: 23066428]
- MacKerell AD Jr, Bashford D, Bellott, Dunbrack RL, Evanseck JD, Field MJ, Fischer S, Gao J, Guo H, Ha S, Joseph-McCarthy D, Kuchnir L, Kuczera K, Lau FTK, Mattos C, Michnick S, Ngo T, Nguyen DT, Prodhom B, Reiher WE, Roux B, Schlenkrich M, Smith JC, Stote R, Straub J, Watanabe M, Wiórkiewicz-Kuczera J, Yin D, Karplus M. All-Atom Empirical Potential for Molecular Modeling and Dynamics Studies of Proteins. *J Phys Chem B.* 1998; 102:3586–3616. [PubMed: 24889800]
- Brooks BR, Brooks CL III, MacKerell AD Jr, Nilsson L, Petrella RJ, Roux B, Won Y, Archontis G, Bartels C, Boresch S, Caflisch A, Caves L, Cui Q, Dinner AR, Feig M, Fischer S, Gao J, Hodoseck M, Im W, Kuczera K, Lazaridis T, Ma J, Ovchinnikov V, Paci E, Pastor RW, Post CB, Pu JZ, Schaefer M, Tidor B, Venable RM, Woodcock HL, Wu X, Yang W, York DM, Karplus M. CHARMM: The biomolecular simulation program. *J Comput Chem.* 2009; 30:1545–1614. [PubMed: 19444816]
- Phillips JC, Braun R, Wang W, Gumbart J, Tajkhorshid E, Villa E, Chipot C, Skeel RD, Kalé L, Schulten K. Scalable Molecular Dynamics with NAMD. *J Comput Chem.* 2005; 26:1781–1802. [PubMed: 16222654]
- Jiang W, Hardy DJ, Phillips JC, MacKerell AD Jr, Schulten K, Roux B. High-Performance Scalable Molecular Dynamics Simulations of a Polarizable Force Field Based on Classical Drude Oscillators in NAMD. *J Phys Chem Lett.* 2011; 2:87–92. [PubMed: 21572567]
- Lemkul JA, Roux B, van der Spoel D, MacKerell AD Jr. Implementation of Extended Lagrangian Dynamics in GROMACS for Polarizable Simulations Using the Classical Drude Oscillator Model. *J Comput Chem.* 2015; 36:1473–1479. [PubMed: 25962472]
- Abraham MJ, Murtola T, Schulz R, Páll S, Smith JC, Hess B, Lindahl E. GROMACS: High performance molecular simulations through multi-level parallelism from laptops to supercomputers. *SoftwareX.* 2015; 1–2:19–25.

17. Huang J, Lemkul JA, Eastman PK, MacKerell AD Jr. Molecular Dynamics Simulations of Explicitly Solvated Drude Polarizable Systems on GPUs: Implementation, Validation, and Benchmark. *J Comput Chem*. 2018 In press.
18. Lamoureux G, MacKerell AD Jr, Roux B. A simple polarizable model of water based on classical Drude oscillators. *J Chem Phys*. 2003; 119:5185–5197.
19. Lamoureux G, Harder E, Vorobyov IV, Roux B, MacKerell AD Jr. A polarizable model of water for molecular dynamics simulations of biomolecules. *Chem Phys Lett*. 2006; 418:245–249.
20. Yu WB, Lopes PEM, Roux B, MacKerell AD Jr. Six-site polarizable model of water based on the classical Drude oscillator. *J Chem Phys*. 2013; 138:034508. [PubMed: 23343286]
21. Vorobyov IV, Anisimov VM, MacKerell AD Jr. Polarizable Empirical Force Field for Alkanes Based on the Classical Drude Oscillator Model. *J Phys Chem B*. 2005; 109:18988–18999. [PubMed: 16853445]
22. Anisimov VM, Vorobyov IV, Roux B, MacKerell AD Jr. Polarizable Empirical Force Field for the Primary and Secondary Alcohol Series Based on the Classical Drude Model. *J Chem Theory Comput*. 2007; 3:1927–1946. [PubMed: 18802495]
23. Lopes PEM, Lamoureux G, Roux B, MacKerell AD Jr. Polarizable Empirical Force Field for Aromatic Compounds Based on the Classical Drude Oscillator. *J Phys Chem B*. 2007; 111:2873–2885. [PubMed: 17388420]
24. Lopes PEM, Lamoureux G, MacKerell AD Jr. Polarizable empirical force field for nitrogen-containing heteroaromatic compounds based on the classical Drude oscillator. *J Comput Chem*. 2009; 30:1821–1838. [PubMed: 19090564]
25. Vorobyov I, Anisimov VM, Greene S, Venable RM, Moser A, Pastor RW, MacKerell AD Jr. Additive and Classical Drude Polarizable Force Fields for Linear and Cyclic Ethers. *J Chem Theory Comput*. 2007; 3:1120–1133. [PubMed: 26627431]
26. Baker CM, MacKerell AD Jr. Polarizability rescaling and atom-based Thole scaling in the CHARMM Drude polarizable force field for ethers. *J Mol Model*. 2010; 16:567–576. [PubMed: 19705172]
27. Zhu X, MacKerell AD Jr. Polarizable empirical force field for sulfur-containing compounds based on the classical Drude oscillator model. *J Comput Chem*. 2010; 31:2330–2341. [PubMed: 20575015]
28. He X, Lopes PEM, MacKerell AD Jr. Polarizable Empirical Force Field for Acyclic Poly-Alcohols Based on the Classical Drude Oscillator. *Biopolymers*. 2013; 99:724–738. [PubMed: 23703219]
29. Lin F-Y, MacKerell AD Jr. Polarizable Empirical Force Field for Halogen-Containing Compounds Based on the Classical Drude Oscillator. *J Chem Theory Comput*. 2018; 14:1083–1098. [PubMed: 29357257]
30. Harder E, Anisimov VM, Whitfield T, MacKerell AD Jr, Roux B. Understanding the Dielectric Properties of Liquid Amides from a Polarizable Force Field. *J Phys Chem B*. 2008; 112:3509–3521. [PubMed: 18302362]
31. Lin B, Lopes PEM, Roux B, MacKerell AD Jr. Kirkwood-Buff analysis of aqueous N-methylacetamide and acetamide solutions modeled by the CHARMM additive and Drude polarizable force fields. *J Chem Phys*. 2013; 139:084509. [PubMed: 24007020]
32. Lopes PEM, Huang J, Shim J, Luo Y, Li H, Roux B, MacKerell AD Jr. Polarizable Force Field for Peptides and Proteins Based on the Classical Drude Oscillator. *J Chem Theory Comput*. 2013; 9:5430–5449. [PubMed: 24459460]
33. Chowdhary J, Harder E, Lopes PEM, Huang L, MacKerell AD Jr, Roux B. A Polarizable Force Field of Dipalmitoylphosphatidylcholine Based on the Classical Drude Model for Molecular Dynamics Simulations of Lipids. *J Phys Chem B*. 2013; 117:9142–9160. [PubMed: 23841725]
34. Li H, Chowdhary J, Huang L, He X, MacKerell AD Jr, Roux B. Drude Polarizable Force Field for Molecular Dynamics Simulations of Saturated and Unsaturated Zwitterionic Lipids. *J Chem Theory Comput*. 2017; 13:4535–4552. [PubMed: 28731702]
35. Jana M, MacKerell AD Jr. CHARMM Drude Polarizable Force Field for Aldopentofuranoses and Methyl-aldopentofuranosides. *J Phys Chem B*. 2015; 119:7846–7859. [PubMed: 26018564]

36. Small MC, Aytenfisu AH, Lin F-Y, He X, MacKerell AD Jr. Drude polarizable force field for aliphatic ketones and aldehydes, and their associated acyclic carbohydrates. *J Comput Aided Mol Des.* 2017; 31:349–363. [PubMed: 28190218]
37. Yang M, Aytenfisu AH, MacKerell AD Jr. Proper balance of solvent-solute and solute-solute interactions in the treatment of the diffusion of glucose using the Drude polarizable force field. *Carbohydr Res.* 2018; 457:41–50. [PubMed: 29422120]
38. Baker CM, Anisimov VM, MacKerell AD Jr. Development of CHARMM Polarizable Force Field for Nucleic Acid Bases Based on the Classical Drude Oscillator Model. *J Phys Chem B.* 2011; 115:580–596. [PubMed: 21166469]
39. Savelyev A, MacKerell AD Jr. All-atom polarizable force field for DNA based on the classical drude oscillator model. *J Comput Chem.* 2014; 35:1219–1239. [PubMed: 24752978]
40. Lemkul JA, MacKerell AD Jr. Polarizable Force Field for DNA Based on the Classical Drude Oscillator: I. Refinement Using Quantum Mechanical Base Stacking and Conformational Energetics. *J Chem Theory Comput.* 2017; 13:2053–2071. [PubMed: 28399366]
41. Lemkul JA, MacKerell AD Jr. Polarizable Force Field for DNA Based on the Classical Drude Oscillator: II. Microsecond Molecular Dynamics Simulations of Duplex DNA. *J Chem Theory Comput.* 2017; 13:2072–2085. [PubMed: 28398748]
42. Yu H, Whitfield TW, Harder E, Lamoureux G, Vorobyov I, Anisimov VM, MacKerell AD Jr, Roux B. Simulating Monovalent and Divalent Ions in Aqueous Solution Using a Drude Polarizable Force Field. *J Chem Theory Comput.* 2010; 6:774–786. [PubMed: 20300554]
43. Lemkul JA, Huang J, Roux B, MacKerell AD Jr. An Empirical Polarizable Force Field Based on the Classical Drude Oscillator Model: Development History and Recent Applications. *Chem Rev.* 2016; 116:4983–5013. [PubMed: 26815602]
44. Baker CM, Lopes PEM, Zhu X, Roux B, MacKerell AD Jr. Accurate Calculation of Hydration Free Energies using Pair-Specific Lennard-Jones Parameters in the CHARMM Drude Polarizable Force Field. *J Chem Theory Comput.* 2010; 6:1181–1198. [PubMed: 20401166]
45. Turney JM, Simmonett AC, Parrish RM, Hohenstein EG, Evangelista FA, Fermann JT, Mintz BJ, Burns LA, Wilke JJ, Abrams ML, Russ NJ, Leininger ML, Janssen CL, Seidl ET, Allen WD, Schaefer HF, King RA, Valeev EF, Sherrill CD, Crawford TD. Psi4: an open-source ab initio electronic structure program. *WIREs Comput Mol Sci.* 2012; 2:556–565.
46. Frisch MJ, Trucks GW, Schlegel HB, Scuseria GE, Robb MA, Cheeseman JR, Montgomery JA, Vreven T, Kudin KN, Burant JC, Millam JM, Iyengar SS, Tomasi J, Barone V, Mennucci B, Cossi M, Scalmani G, Rega N, Petersson GA, Nakatsuji H, Hada M, Ehara M, Toyota K, Fukuda R, Hasegawa J, Ishida M, Nakajima T, Honda Y, Kitao O, Nakai H, Klene M, Li X, Knox JE, Hratchian HP, Cross JB, Bakken V, Adamo C, Jaramillo J, Gomperts R, Stratmann RE, Yazyev O, Austin AJ, Cammi R, Pomelli C, Ochterski JW, Ayala PY, Morokuma K, Voth GA, Salvador P, Dannenberg JJ, Zakrzewski VG, Dapprich S, Daniels AD, Strain MC, Farkas O, Malick DK, Rabuck AD, Raghavachari K, Foresman JB, Ortiz JV, Cui Q, Baboul AG, Clifford S, Cioslowski J, Stefanov BB, Liu G, Liashenko A, Piskorz P, Komaromi I, Martin RL, Fox DJ, Keith T, Laham A, Peng CY, Nanayakkara A, Challacombe M, Gill PMW, Johnson B, Chen W, Wong MW, Gonzalez C, Pople JA. *Gaussian 03: Revision C.02.* 2003
47. NIST Computational Chemistry Comparison and Benchmark Database. [accessed Oct 8: 2017] NIST Standard Reference Database Number 101 Release 18. <http://cccbdb.nist.gov>
48. Scott AP, Radom L. Harmonic Vibrational Frequencies: An Evaluation of Hartree–Fock, Møller–Plesset, Quadratic Configuration Interaction, Density Functional Theory, and Semiempirical Scale Factors. *The Journal of Physical Chemistry.* 1996; 100:16502–16513.
49. Pulay P, Fogarasi G, Pang F, Boggs JE. Systematic ab initio gradient calculation of molecular geometries, force constants, and dipole moment derivatives. *J Am Chem Soc.* 1979; 101:2550–2560.
50. Becke AD. Density-functional exchange-energy approximation with correct asymptotic behavior. *Phys Rev A.* 1988; 38:3098–3100.
51. Becke AD. Density-functional thermochemistry. III. The role of exact exchange. *J Chem Phys.* 1993; 98:5648–5652.

52. Lee C, Yang W, Parr RG. Local softness and chemical reactivity in the molecules CO, SCN⁻ and H₂CO. *J Mol Struct.* 1988; 163:305–313.
53. Dunning TH. Gaussian basis sets for use in correlated molecular calculations. I. The atoms boron through neon and hydrogen. *J Chem Phys.* 1989; 90:1007–1023.
54. Bernardi F, Boys SF. Explicit formula solutions of the contraction conditions for transcorrelated wavefunctions. *Mol Phys.* 1973; 25:35–44.
55. Vanommeslaeghe K, Hatcher E, Acharya C, Kundu S, Zhong S, Shim J, Darian E, Guvench O, Lopes P, Vorobyov I, MacKerell AD Jr. CHARMM General Force Field (CGenFF): A force field for drug-like molecules compatible with the CHARMM all-atom additive biological force fields. *J Comput Chem.* 2010; 31:671–690. [PubMed: 19575467]
56. Jorgensen WL, Chandrasekhar J, Madura JD, Impey RW, Klein ML. Comparison of simple potential functions for simulating liquid water. *J Chem Phys.* 1983; 79:926–935.
57. Kollman PA. Free energy calculations: Applications to chemical and biochemical phenomena. *Chem Rev.* 1993; 93:2395–2417.
58. Lamoureux G, Roux B. Modeling induced polarization with classical Drude oscillators: Theory and molecular dynamics simulation algorithm. *J Chem Phys.* 2003; 119:3025.
59. Essmann U, Perera L, Berkowitz ML, Darden T, Lee H, Pedersen LG. A smooth particle mesh Ewald method. *J Chem Phys.* 1995; 103:8577–8593.
60. Brooks BR, Bruccoleri RE, Olafson DJ, States DJ, Swaminathan S, Karplus M. CHARMM: A Program for Macromolecular Energy, Minimization, and Dynamics Calculations. *J Comput Chem.* 1983; 4:187–217.
61. Steinbach PJ, Brooks BR. New spherical-cutoff methods for long-range forces in macromolecular simulation. *J Comput Chem.* 1994; 15:667–683.
62. Nosé S. A unified formulation of the constant temperature molecular dynamics methods. *J Chem Phys.* 1984; 81:511–519.
63. Hoover WG. Canonical dynamics: Equilibrium phase-space distributions. *Phys Rev A.* 1985; 31:1695–1697.
64. Martyna GJ, Tobias DJ, Klein ML. Constant pressure molecular dynamics algorithms. *J Chem Phys.* 1994; 101:4177–4189.
65. Ryckaert J-P, Ciccotti G, Berendsen HJC. Numerical integration of the cartesian equations of motion of a system with constraints: molecular dynamics of n-alkanes. *J Comput Phys.* 1977; 23:327–341.
66. Martyna GJ, Tuckerman ME, Tobias DJ, Klein ML. Explicit reversible integrators for extended systems dynamics. *Mol Phys.* 1996; 87:1117–1157.
67. Lin Y-L, Aleksandrov A, Simonson T, Roux B. An Overview of Electrostatic Free Energy Computations for Solutions and Proteins. *J Chem Theory Comput.* 2014; 10:2690–2709. [PubMed: 26586504]
68. Simonson T, Hummer G, Roux B. Equivalence of M- and P-Summation in Calculations of Ionic Solvation Free Energies. *J Phys Chem A.* 2017; 121:1525–1530. [PubMed: 28152306]
69. Lamoureux G, Roux B. Absolute Hydration Free Energy Scale for Alkali and Halide Ions Established from Simulations with a Polarizable Force Field. *J Phys Chem B.* 2006; 110:3308–3322. [PubMed: 16494345]
70. Asthagiri D, Pratt LR, Ashbaugh HS. Absolute hydration free energies of ions, ion–water clusters, and quasichemical theory. *J Chem Phys.* 2003; 119:2702–2708.
71. Harder E, Roux B. On the origin of the electrostatic potential difference at a liquid-vacuum interface. *J Chem Phys.* 2008; 129:234706. [PubMed: 19102551]
72. Kastenholz MA, Hünenberger PH. Computation of methodology-independent ionic solvation free energies from molecular simulations. I. The electrostatic potential in molecular liquids. *J Chem Phys.* 2006; 124:124106. [PubMed: 16599661]
73. Kastenholz MA, Hünenberger PH. Computation of methodology-independent ionic solvation free energies from molecular simulations. II. The hydration free energy of the sodium cation. *J Chem Phys.* 2006; 124:224501. [PubMed: 16784292]

74. Deng Y, Roux B. Hydration of Amino Acid Side Chains: Nonpolar and Electrostatic Contributions Calculated from Staged Molecular Dynamics Free Energy Simulations with Explicit Water Molecules. *J Phys Chem B*. 2004; 108:16567–16576.
75. Kumar S, Rosenberg JM, Bouzida D, Swendsen RH, Kollman PA. The weighted histogram analysis method for free-energy calculations on biomolecules. I. The method. *J Comput Chem*. 1992; 13:1011–1021.
76. Lagüe P, Pastor RW, Brooks BR. Pressure-Based Long-Range Correction for Lennard-Jones Interactions in Molecular Dynamics Simulations: Application to Alkanes and Interfaces. *J Phys Chem B*. 2004; 108:363–368.
77. Pliego JR, Riveros JM. Gibbs energy of solvation of organic ions in aqueous and dimethyl sulfoxide solutions. *Phys Chem Chem Phys*. 2002; 4:1622–1627.
78. Canuto, S. *Solvation Effects on Molecules and Biomolecules - Computational Methods and Applications*. 1. Springer; Netherlands: 2008.
79. Reif MM, Hünenberger PH, Oostenbrink C. New Interaction Parameters for Charged Amino Acid Side Chains in the GROMOS Force Field. *J Chem Theory Comput*. 2012; 8:3705–3723. [PubMed: 26593015]
80. Vorobyov I, Li L, Allen TW. Assessing Atomistic and Coarse-Grained Force Fields for Protein–Lipid Interactions: the Formidable Challenge of an Ionizable Side Chain in a Membrane. *J Phys Chem B*. 2008; 112:9588–9602. [PubMed: 18636764]
81. Kelly CP, Cramer CJ, Truhlar DG. Aqueous Solvation Free Energies of Ions and Ion–Water Clusters Based on an Accurate Value for the Absolute Aqueous Solvation Free Energy of the Proton. *J Phys Chem B*. 2006; 110:16066–16081. [PubMed: 16898764]
82. Hofer TS, Hünenberger PH. Absolute proton hydration free energy, surface potential of water, and redox potential of the hydrogen electrode from first principles: QM/MM MD free-energy simulations of sodium and potassium hydration. *J Chem Phys*. 2018; 148:222814.
83. Jo S, Kim T, Iyer VG, Im W. CHARMM-GUI: A web-based graphical user interface for CHARMM. *J Comput Chem*. 2008; 29:1859–1865. [PubMed: 18351591]
84. Anisimov VM, Lamoureux G, Vorobyov IV, Huang N, Roux B, MacKerell AD Jr. Determination of Electrostatic Parameters for a Polarizable Force Field Based on the Classical Drude Oscillator. *J Chem Theory Comput*. 2005; 1:153–168. [PubMed: 26641126]
85. Harder E, Anisimov VM, Vorobyov IV, Lopes PEM, Noskov SY, MacKerell AD Jr, Roux B. Atomic Level Anisotropy in the Electrostatic Modeling of Lone Pairs for a Polarizable Force Field Based on the Classical Drude Oscillator. *J Chem Theory Comput*. 2006; 2:1587–1597. [PubMed: 26627029]
86. Miller KJ. Additivity methods in molecular polarizability. *J Am Chem Soc*. 1990; 112:8533–8542.
87. Yin D, MacKerell AD Jr. Combined ab initio/empirical approach for optimization of Lennard–Jones parameters. *J Comput Chem*. 1998; 19:334–348.
88. Foloppe N, MacKerell JAD. All-atom empirical force field for nucleic acids: I. Parameter optimization based on small molecule and condensed phase macromolecular target data. *J Comput Chem*. 2000; 21:86–104.
89. MacKerell, AD., Jr, Brooks, B., Brooks, CL., III, Nilsson, L., Roux, B., Won, Y., Karplus, M. CHARMM: The Energy Function and Its Parameterization with an Overview of the Program. In: Schleyer, PvR, editor. *Encyclopedia of computational chemistry*. New York: J. Wiley: Chichester; 1998.
90. Beglov D, Roux B. Finite representation of an infinite bulk system: Solvent boundary potential for computer simulations. *J Chem Phys*. 1994; 100:9050–9063.
91. Gallicchio E, Paris K, Levy RM. The AGBNP2 Implicit Solvation Model. *J Chem Theory Comput*. 2009; 5:2544–2564. [PubMed: 20419084]
92. Cabani S, Gianni P, Mollica V, Lepori L. Group contributions to the thermodynamic properties of non-ionic organic solutes in dilute aqueous solution. *J Solution Chem*. 1981; 10:563–595.
93. Kelly CP, Cramer CJ, Truhlar DG. SM6: A Density Functional Theory Continuum Solvation Model for Calculating Aqueous Solvation Free Energies of Neutrals, Ions, and Solute–Water Clusters. *J Chem Theory Comput*. 2005; 1:1133–1152. [PubMed: 26631657]

94. Li P, Merz KM. Metal Ion Modeling Using Classical Mechanics. *Chem Rev.* 2017; 117:1564–1686. [PubMed: 28045509]

Author Manuscript

Author Manuscript

Author Manuscript

Author Manuscript

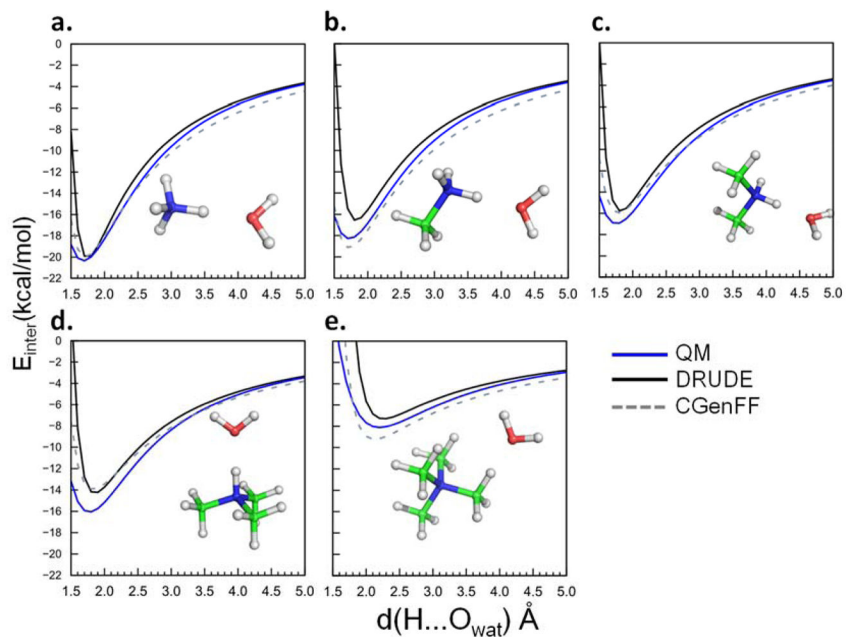


Figure 1.

Water interaction energy surfaces as a function of distance from the QM, Drude and additive (CGenFF) models with ammonium (NH₄), methylammonium (NC1), dimethylammonium (NC2), trimethylammonium (NC3), and tetramethylammonium (NC4) in **a.** to **e.**, respectively. Distances are labeled between the hydrogen (H) on the model compounds and water oxygen (O_{water}). Carbons are label in green, nitrogens in blue, oxygen in red, and hydrogens in white.

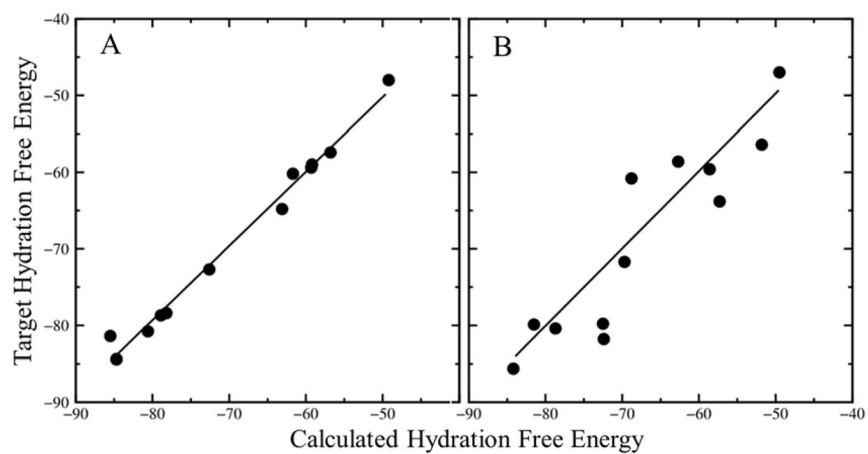


Figure 2. Correlation plots of the calculated and target hydration free energies (kcal/mol) for the A) Drude polarizable and B) CGenFF additive force fields. Regression lines are shown where $y = 0.970x - 1.7222$ ($R^2 = 0.99$) for the Drude and $y = 1.012x - 0.6651$ ($R^2 = 0.84$) for the CGenFF force fields.

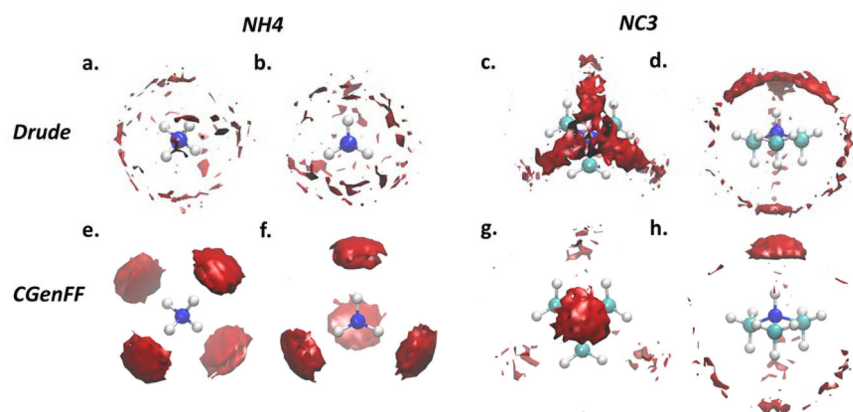


Figure 3. Spatial probability distributions of water molecules in the vicinity of ammonium (NH₄) and trimethylammonium (NC₃). Drude model of NH₄ viewed from orthogonal perspectives are shown in **a–b** and for NC₃ in **c–d**. Corresponding distributions for the additive CGenFF model of NH₄ and NC₃ are shown in **e–h**. Probabilities are calculated through $n_{\text{water_atoms}}/N$, where $n_{\text{water_atom}}$ is the occupancy of water atoms occurring in a voxel of $0.25 \times 0.25 \times 0.25 \text{ \AA}^3$, and N is the total occupancy over all the voxels. Surfaces are drawn to encompass voxels with probability larger than 0.0055.

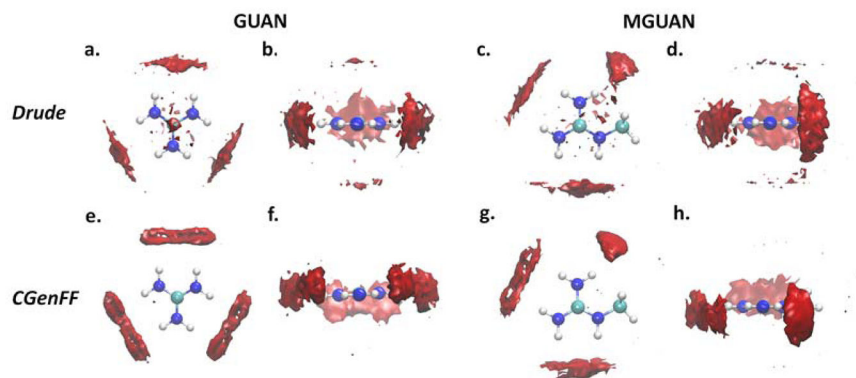


Figure 4. Spatial probability distributions of water molecules in the vicinity of guanidinium (GUAN) and methylguanidinium (MGUAN). Drude model of GUAN viewed from orthogonal perspectives are shown in **a–b** and for MGUAN in **c–d**. Corresponding distributions for the additive CGenFF model of GUAN and MGUAN are shown in **e–h**. Probabilities are calculated through $n_{\text{water_atoms}}/N$, where $n_{\text{water_atom}}$ is the occupancy of water atoms occurring in a voxel of $0.25 \times 0.25 \times 0.25 \text{ \AA}^3$, and N is the total occupancy over all the voxels. Surfaces are drawn to encompass voxels with probability larger than 0.0055.

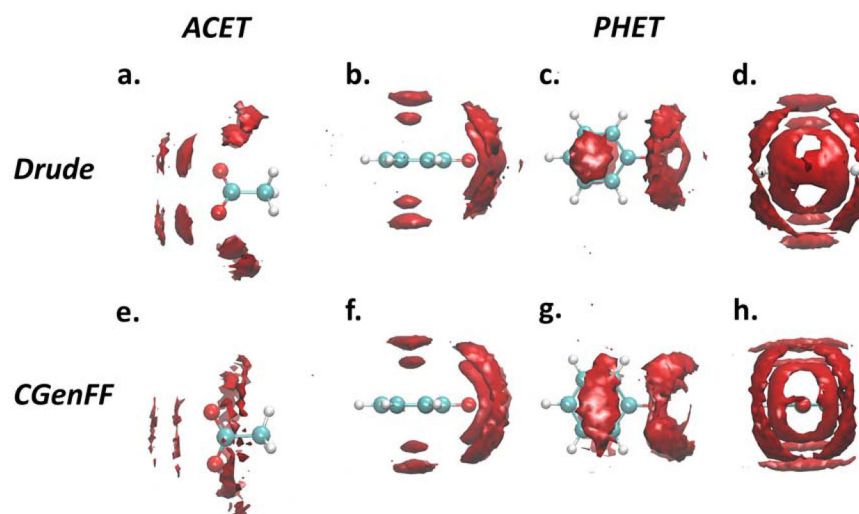


Figure 5. Spatial probability distributions of water molecules in the vicinity of acetate (ACET) and phenolate (PHET). Drude model of ACET viewed from orthogonal perspectives are shown in **a–b** and for PHET in **c–d**. Corresponding distributions for the additive CGenFF model of ACET and PHET are shown in **e–h**. Probabilities are calculated through $n_{\text{water_atoms}}/N$, where $n_{\text{water_atom}}$ is the occupancy of water atoms occurring in a voxel of $0.25 \times 0.25 \times 0.25 \text{ \AA}^3$, and N is the total occupancy over all the voxels. Surfaces are drawn to encompass voxels with probability larger than 0.0055.

Table 1

Abbreviations of the molecular ions studied in this work.

Molecule names	Abbreviations
Ammonium	NH ₄
Methylammonium	NC1
Dimethylammonium	NC2
Trimethylammonium	NC3
Tetramethylammonium	NC4
Imidazolium	IMIM
Guanidinium	GUAN
Methylguanidinium	MGUAN
Acetate	ACET
Methanethiolate	MES
Ethanethiolate	ETS
Phenolate	PHET

Author Manuscript

Author Manuscript

Author Manuscript

Author Manuscript

Table 2

Hydration free energy (G_{hyd} , kcal/mol) of Cl^- and Na^+ and reference H^+ used in the development of the Drude monoatomic ions.⁴²

$\text{X}^{+/-}$	Cl^-	Na^+	H^+
G_{hyd}	-78.4	-96.3	-258.8

Author Manuscript

Author Manuscript

Author Manuscript

Author Manuscript

Table 3

Target hydration free energies $G(Y^{-/+}_{\text{target}})$ for the respective molecular ions ($Y^{-/+}$) and their counterion ($X^{-/+}$) used for the Drude polarizable force field.

Molecule ($Y^{-/+}$)	($X^{-/+}$)	$G(Y^{-/+}_{\text{ref}})$	$G(X^{-/+}_{\text{ref}})$	$G(X^{-/+}_{\text{Drude}})$	$G(Y^{-/+}_{\text{target}})$	Method ^a
NH4	Chloride	-85.2 ⁷⁷ .81	-74.6 ⁷⁶ .80	-78.4 ⁴²	-81.4 ± 2.0 ⁷⁷ .81	2
NC1	Chloride	-76.5 ⁷⁶ .80	-74.6 ⁷⁶ .80	-78.4 ⁴²	-72.7 ± 2.0 ⁷⁷ .81	2
NC2	Chloride	-68.6 ⁷⁶ .80	-74.6 ⁷⁶ .80	-78.4 ⁴²	-64.8 ± 2.0 ⁷⁷ .81	2
NC3	Chloride	-61.2 ⁷⁶ .80	-74.6 ⁷⁶ .80	-78.4 ⁴²	-57.4 ± 2.0 ⁷⁷ .81	2
NC4	Chloride	-50.4 ⁷⁸	-76.0 ⁷⁸	-78.4 ⁴²	-48.0 ⁷⁸ . <i>b</i>	2
IMIM	Proton	-63.1 ⁷⁹	-262.9 ⁷⁹	-258.8 ⁴²	-59.0 ± 1.9 ⁷⁹	1
GUAN	Proton	-64.3 ⁷⁹	-262.9 ⁷⁹	-258.8 ⁴²	-60.2 ⁷⁹ . <i>b</i>	1
MGUAN	Proton	-62.0 ⁸⁰	-261.4 ⁸⁰	-258.8 ⁴²	-59.4 ⁷⁹ . <i>b</i>	1
ETS	Sodium	-71.8 ⁷⁷ .81	-103.2 ⁷⁷ .81	-96.3 ⁴²	-78.7 ± 2.0 ⁷⁷ .81	2
MES	Proton	-73.7 ⁷⁷ .81	-265.9 ⁷⁷ .81	-258.8 ⁴²	-80.8 ± 2.0 ⁷⁷ .81	2
ACET	Proton	-77.3 ⁷⁷ .81	-265.9 ⁷⁷ .81	-258.8 ⁴²	-84.4 ± 2.0 ⁷⁷ .81	2
PHET	Proton	-71.3 ⁷⁷ .81	-265.9 ⁷⁷ .81	-258.8 ⁴²	-78.4 ± 2.0 ⁷⁷ .81	2

^aMethod 1: $G(Y^{-/+}_{\text{target}}) = G(X^{-/+}_{\text{Drude}}) + G(Y^{-/+}_{\text{ref}}) - G(X^{-/+}_{\text{ref}})$.

Method 2: $G(Y^{-/+}_{\text{target}}) = G(X^{-/+}_{\text{ref}}) + G(Y^{-/+}_{\text{ref}}) - G(X^{-/+}_{\text{Drude}})$

^bUncertainties were not provided.

Table 4

Average differences (AVG), absolute unsigned error (AUE), and root-mean-square differences (RMSD) of the computed water minimum interaction energies (E_{\min} , kcal/mol) and distances (R , Å) from Drude model (Drude) and additive model (CGenFF) compared to their QM values for all the molecular ions. Individual interaction results are shown in Table S2. The errors for the averages are the standard deviations.

	Drude		CGenFF	
	E_{\min}	R	E_{\min}	R
AVG	0.37±0.86	0.1±0.1	-0.23±1.34	0.0±0.2
AUE	0.74	0.1	1.09	0.1
RMSD	0.92	0.1	1.34	0.2

Table 5

Dipole moments and molecular polarizabilities computed from the Drude model (Drude) and the additive model (CGenFF) compared to the target QM data. QM Dipoles and molecular polarizabilities were computed based on MP2/cc-pVQZ//MP2/aug-cc-pVDZ model chemistry.

Dipole moment (D)			
Molecule	QM	Drude	CGenFF
NH4	0.00	0.00	0.00
NC1	2.18	2.17	2.71
NC2	1.48	1.53	0.73
NC3	0.86	1.04	0.12
NC4	0.00	0.00	0.00
IMIM	1.27	1.34	0.86
GUAN	0.00	0.00	0.00
MGUAN	1.35	1.35	1.77
ACET	3.57	3.69	4.75
ETS	4.63	4.56	4.63
MES	3.03	2.85	2.19
PHET	4.44	4.65	7.20

Table 6

Molecular polarizability tensors from the QM and Drude models with the ratio of the Drude/QM values.^a

Name	QM			Drude			Total	$\frac{\text{Drude}_{\text{Total}}}{\text{QM}_{\text{Total}}}$
	XX	YY	ZZ	XX	YY	ZZ		
NH4	1.33	1.33	1.33	1.51	1.51	1.51	1.51	1.13
NC1	3.09	2.90	2.91	2.68	2.76	3.23	2.89	0.97
NC2	4.24	5.21	4.42	4.62	5.44	4.05	4.43	0.96
NC3	6.59	6.59	5.63	6.27	6.91	3.92	5.90	0.94
NC4	7.91	7.91	7.91	7.43	7.44	7.43	7.43	0.94
IMIM	3.92	7.01	7.60	6.17	7.40	3.91	6.18	1.00
GUAN	5.96	5.96	3.39	5.10	4.90	3.44	4.41	0.86
MGUAN	7.22	8.63	4.82	6.89	6.06	4.81	5.89	0.85
ACET	6.53	6.41	4.29	5.75	5.16	3.38	4.86	0.85
ETS	11.01	7.77	7.00	8.59	7.14	4.46	5.10	0.59
MES	5.21	5.21	7.91	6.11	3.01	4.98	3.67	0.60
PHET	13.81	16.54	6.92	12.42	8.39	4.55	7.92	0.64

^aQM values from Gaussian are in units of a.u. They were multiplied by 0.1482 to convert to units of Å

Table 7

RMS differences between Drude model geometries and QM target data for all the intramolecular bond lengths (\AA) and angles ($^\circ$).

Molecule	NH4	NC1	NC2	NC3
BOND	0.002	0.011	0.013	0.014
ANGLE	0.000	2.033	1.931	1.689
Molecule	NC4	IMIM	GUAN	MGUAN
BOND	0.016	0.008	0.012	0.015
ANGLE	1.548	1.212	0.696	1.363
Molecule	ACET	MES	ETS	PHET
BOND	0.006	0.008	0.013	0.017
ANGLE	0.848	0.331	1.966	1.714

Author Manuscript

Author Manuscript

Author Manuscript

Author Manuscript

Table 8

Average differences (AVG), absolute unsigned error (AUE), root-mean-square differences (RMSD) and Pearson correlation coefficient squared (R^2) between the calculated and target hydration free energies, G_{hyd} , for the Drude model (Drude) and additive model (CGenFF) compared to their QM values for all the molecular ions. Individual interaction results are shown in Table S2. The errors for the averages are the standard deviations.

	Drude	Drude*	CGenFF	CGenFF*
AVG	-0.38±1.42	-0.05±0.85	1.48±5.03	1.45±5.28
AUG	0.87	0.57	4.18	4.40
RMSD	1.41	0.81	5.04	5.24
R^2	0.99	1.00	0.84	0.83

* Analysis with NH4 results omitted.

Table 9

Simulated ($G_{\text{hyd}}^{\text{real}}$) and target hydration free energies (G_{hyd}) for the studied molecular ions with the Drude and Additive models (kcal/mol). The errors for $G_{\text{hyd}}^{\text{real}}$ are the standard errors (SE) obtained from three independent simulations, where $SE = SD/\sqrt{n}$, SD is the standard deviation and $n = 3$.

Drude Molecular ion	$G_{\text{hyd, Drude}}^{\text{real, a}}$	Target	$G_{\text{hyd, Drude}}^b$	Difference
NH4 ^c	-85.5 ± 0.1	-81.4 ± 2.0 ^{77, 81}		-4.1
NC1	-72.6 ± 0.0	-72.7 ± 2.0 ^{77, 81}		0.1
NC2	-63.1 ± 0.1	-64.8 ± 2.0 ^{77, 81}		1.7
NC3	-56.8 ± 0.1	-57.4 ± 2.0 ^{77, 81}		0.6
NC4	-49.2 ± 0.1	-48.0 ^{78, d}		-1.2
IMIM	-59.2 ± 0.1	-59.0 ± 1.9 ⁷⁹		-0.2
GUAN	-61.7 ± 0.0	-60.2 ^{79, d}		-1.5
MGUAN	-59.3 ± 0.1	-59.4 ^{80, d}		0.1
ETS	-78.9 ± 0.1	-78.7 ± 2.0 ^{77, 81}		-0.2
MES	-80.6 ± 0.1	-80.8 ± 2.0 ^{77, 81}		0.2
ACET	-84.7 ± 0.1	-84.4 ± 2.0 ^{77, 81}		-0.3
PHET	-78.2 ± 0.0	-78.4 ± 2.0 ^{77, 81}		0.2
CGenFF	$G_{\text{hyd, CGenFF}}^{\text{real, a}}$	Target	$G_{\text{hyd, CGenFF}}^e$	Difference
NH4	-78.7 ± 0.1	-80.4 ± 2.0 ^{77, 81, 90}		1.7
NC1	-69.7 ± 0.1	-71.7 ± 2.0 ^{77, 81, 90}		2.0
NC2	-57.3 ± 0.1	-63.8 ± 2.0 ^{77, 81, 90}		6.5
NC3	-51.8 ± 0.0	-56.4 ± 2.0 ^{77, 81, 90}		4.6
NC4	-49.5 ± 0.0	-47.0 ^{78, 90, d}		-2.5
IMIM	-58.6 ± 0.1	-59.6 ± 1.9 ^{79, d}		1.0
GUAN	-68.8 ± 0.1	-60.8 ± 1.9 ^{79, d}		-8.0
MGUAN	-62.7 ± 0.1	-58.6 ^{91, 92, d}		-4.1
ETS	-72.5 ± 0.1	-79.8 ± 2.0 ^{81, 90, 93}		7.3
MES	-72.4 ± 0.1	-81.8 ± 2.0 ^{81, 90, 93}		9.4
ACET	-84.2 ± 0.1	-85.6 ± 2.0 ^{81, 90, 93}		1.4
PHET	-81.5 ± 0.2	-79.9 ± 2.0 ^{81, 90, 93}		-1.6

^aAir/water interface potential of SWM4-NDP water: $\phi = -545$ mV and $zF\phi = \pm 12.6$ kcal/mol.¹⁹ Air/water interface potential of TIP3P water: $\phi = -500$ mV and $zF\phi = \pm 11.5$ kcal/mol.⁶⁹

^bThe reference hydration free energies for the monoatomic ions Cl^- , Na^+ or H^+ (G_{hyd}) optimized for the Drude⁴² are used to normalize the hydration free energies for the respective molecular ions reported in the literature.^{77–81}

^cSpecific NH4 nitrogen LJ parameters $\epsilon = -0.025$, $R_{\text{min}}/2 = 1.76$, yield $G_{\text{hyd}}^{\text{real}}$ of -81.3 ± 0.0 kcal/mol, in significantly improved agreement with the experimental value.

^dUncertainties were not provided.

^eDetails of the calculation for the additive target Ghyd, CGenFF are presented in Table S1.

Author Manuscript

Author Manuscript

Author Manuscript

Author Manuscript